

**UNIVERSITY OF PARDUBICE**  
**FACULTY OF CHEMICAL TECHNOLOGY**  
Institute of Organic Chemistry and Technology

**Ing. Jan Podlesný**

**Conjugated compounds based on condensed thiophene  
derivatives**

*Theses of the Doctoral Dissertation*

Pardubice 2019

Study program: **Organic Chemistry**

Study field: **Organic Chemistry**

Author: **Ing. Jan Podlesný**

Supervisor: **prof. Ing. Filip Bureš, Ph.D.**

Year of the defence: 2019

## References

PODLESNÝ, Jan, *Fused Thiophene Derivatives and Their Utilization in Optoelectronics*, Pardubice, 2019. 163 pages. Dissertation thesis (Ph.D.). University of Pardubice, Faculty of Chemical Technology, Institute of Organic Chemistry and Technology. Supervisor prof. Ing. Filip Bureš, Ph.D.

## Abstract

A literature search focused on synthetic pathways leading to thieno[3,2-*b*]thiophene, thieno[3,2-*b*]thiophene and 4*H*-cyclopenta[*c*]thiophen-4,6(5*H*)-dione has been performed within the scope of this dissertation work. The literature search also covers symmetrical structural modifications of both thienothiophene isomers in the positions 2 and 5. The final part of the literature search focuses on potential applications of the aforementioned heterocyclic compounds in various optoelectronics. Fourteen new D- $\pi$ -A push-pull chromophores divided into two series were synthesized within the experimental part. Both series differ in used thienothiophene donor. The utilized acceptor units were identical for both series, thus seven structurally analogous pairs of target compounds were prepared. Tuning of the optoelectronic and thermal properties has been realized through variation of the electron-releasing and electron-withdrawing substituent respectively. Indan-1,3-dione, *N,N*-diethylthiobarbiturate, *N,N*-dibutylbarbiturate, 4*H*-cyclopenta[*c*]thiophen-4,6(5*H*)-dione, *N*-butylrhodanine, dicyano- and tricyanovinyl groups were employed as acceptor units. Structure and purity of target chromophores were verified by thin layer chromatography, <sup>1</sup>H and <sup>13</sup>C NMR spectroscopy, HR-MALDI mass spectrometry and elemental analysis. Structure-property relationships were investigated by differential scanning calorimetry, thermogravimetric analysis, electrochemistry, UV-VIS absorption spectroscopy and SHG and THG experiments. The achieved results were also supported by theoretical DFT calculations.

## Keywords

thienothiophene, push-pull chromophore, electron-donor/acceptor, optoelectronic properties, nonlinear optics

## Abstrakt

V rámci této disertační práce byla provedena literární rešerše zaměřená na syntetické postupy vedoucí k thieno[3,2-*b*]thiofenu, thieno[2,3-*b*]thiofenu a 4*H*-cyklopenta[*c*]thiofen-4,6(5*H*)-dionu. Literární rešerše se dále zabývá symetrickými strukturálními modifikacemi obou thienothiofenových izomerů v polohách 2 a 5. Poslední částí literární rešerše je kapitola popisující aplikace výše zmíněných heterocyklických sloučenin v různých oblastech optoelektroniky. V experimentální části této disertační práce bylo syntetizováno celkem 14 nových D- $\pi$ -A push-pull chromoforů rozdělených do dvou sérií v závislosti na výše zmíněném použitém thienothiofenovém donoru. Aplikované akceptorní jednotky byly shodné pro obě série, tudíž vzniklo celkem 7 strukturálně analogických párů cílových sloučenin. Ladění optoelektronických a termálních vlastností chromoforů bylo realizováno prostřednictvím záměny elektron-donorního thienothiofenového resp. elektron-akceptorního substituentu. Mezi využitě akceptorní jednotky patří indan-1,3-dion, *N,N*-diethylthiobarbiturová kyselina, *N,N*-dibutylbarbiturová kyselina, 4*H*-cyklopenta[*c*]thiofen-4,6(5*H*)-dion, *N*-butylrhodanin, dikyan- a trikyanvinyl. Struktura a čistota cílových chromoforů byla ověřena pomocí tenkovrstvé chromatografie, <sup>1</sup>H a <sup>13</sup>C NMR spektroskopie, HR-MALDI hmotnostní spektrometrie a elementární analýzy. Vztahy mezi strukturou a vlastnostmi byly studovány s využitím diferenční skenovací kalorimetrie, termogravimetrické analýzy, elektrochemie, UV-VIS absorpční spektroskopie a pomocí SHG a THG experimentů. Získané výsledky byly rovněž doplněny o teoretické DFT kalkulace.

## Klíčová slova

thienothiofen, push-pull chromofor, elektron-donor/akceptor, optoelektronické vlastnosti, nelineární optika

## Table of Contents

1. Introduction .....	6
2. Aims of thesis.....	9
3. Results and discussion.....	10
3.1. Synthesis.....	10
3.2. Thermal behaviour .....	11
3.3. Electrochemistry.....	12
3.4. Linear optical properties.....	13
3.5. Nonlinear optical properties.....	16
3.6. DFT calculations .....	17
4. Conclusion.....	19
5. List of References .....	21
6. List of Student's Published Works.....	24

## Acknowledgment

I would like to thank my supervisor prof. Ing. Filip Bureš, Ph.D. for all-round help, valuable advices and constructive approach both during my experimental work and during writing of my dissertation and scholarly publications. Further, I would like to thank my friends and colleagues from Organic Materials Unit, Institute of Organic Chemistry and Technology, University of Pardubice for enjoyable and motivating working environment. Namely, I thank to Sylva Hladíková for elemental analysis, to Ing. Milan Klikar, Ph.D. for differential scanning calorimetric and electrochemical measurement, to Ing. Patrik Pařík, Ph.D. for measurement of most NMR spectra, to prof. Ing. Oldřich Pytela, DrSc. for DFT calculations, to Martina Sebránková for UV-VIS spectra measurement and unlimited material support, to Ing. Jiří Tydlitát, Ph.D. for HR-MLADI mass spectra measurement. I would like also to thank prof. Iwan V. Kityk's working group for SHG and THG measurements. Further, I would like to thank National Institute for Material Sciences (NIMS), Tsukuba, Japan and my local supervisor Dr. Yasuhiro Shirai for possibility to spend part of my doctoral studies at a foreign internship.

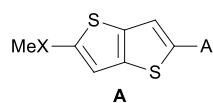
My thanks belong also to my family and friends, who encouraged me during my entire university studies.

Especially, I would like to thank my girlfriend Ing. Veronika Jelínková for help, ideas and great patience during writing of my dissertation.

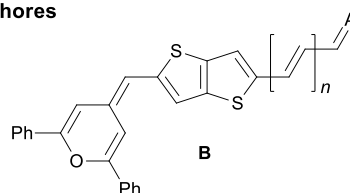
This work was supported from European Regional development Fund-Project "Organic redox couple based batteries for energetics of traditional and renewable resources (ORGBAT)" No.CZ.02.1.01/0.0/0.0/16\_025/0007445.

# 1. Introduction

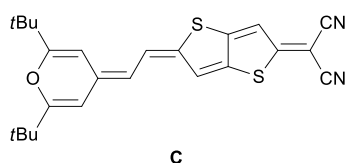
## Known TT-based NLOphores



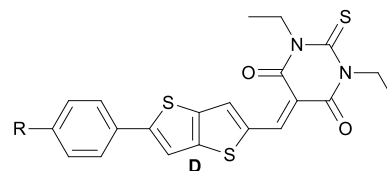
X = O, S, Se, Te; A = CHO, NO<sub>2</sub>, tricyanovinyl  
*J. Chem. Soc. Perkin Trans. 2*, 1996, 1377–1384.



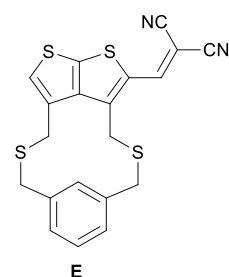
A = thiobarbituric acid, tricyanofuran; n = 1-2  
*Tetrahedron*, 2013, **69**, 3919–3926.



*Org. Biomol. Chem.*, 2013, **11**, 6338–6349.



R = H, OMe, OEt, NEt<sub>2</sub>, pyrrolidino.  
*Eur. J. Org. Chem.*, 2016, **2016**, 5263–5273.



*Tetrahedron Lett.*, 2006, **47**, 5599–5602.

## Investigated TTs

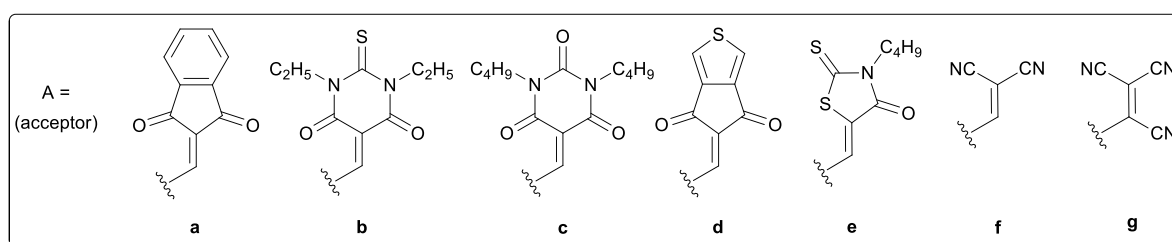
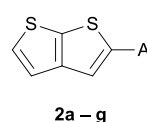
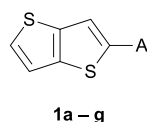


**Figure 1.** Structures of known and investigated TT-derived push-pull derivatives

Thienothiophenes (TT) represent electron-rich bicyclic systems with two annulated thiophene rings that are frequently applied as inherent structural motif of  $\pi$ -conjugated materials for optoelectronics and photonics.<sup>[1]</sup> According to the sulphur atom mutual orientation, four regioisomers can be distinguished from which thieno[3,2-*b*]thiophene and thieno[2,3-*b*]thiophene are the most popular ones. These two heterocyclic scaffolds were firstly mentioned in 1935 and 1886 by Challenger/Harrison<sup>[2]</sup> and Biedermann/Jacobson,<sup>[3]</sup> respectively. In contrast to common single thiophene-derived molecules, TTs brings planar and rigidified  $\pi$ -system that allows

enhanced intramolecular charge transfer (ICT) from/to the appended peripheral substituents. Since thiophene molecules are especially used as semiconductors, light-harvesting or photoluminescent substances, the molecular planarity of TT plays an important role. In D- $\pi$ -A push-pull chromophores, both thieno[3,2-*b*]thiophene and thieno[2,3-*b*]thiophene may act as an auxiliary electron-releasing unit<sup>[4-6]</sup> or a  $\pi$ -linker allowing the ICT between appended donors (D) and acceptors (A).<sup>[7-9]</sup> Moreover, TTs represent planar, extended and polarizable alternative to common  $\pi$ -linkers such as 1,4-phenylene or 2,5-thienylene.<sup>[10]</sup> Due to the aforementioned features, TTs were successfully integrated into functional polymers forming emitting<sup>[11]</sup> or hole injection layer<sup>[12]</sup> of organic light-emitting diodes (OLED) as well as in various types of organic solar cells (OSC). Hence, TT-derived molecules are active electron-donating substances in bulk hetero-junction (BHJ) solar cells,<sup>[13-15]</sup> functional dye in dye sensitized solar cells (DSSC)<sup>[8,16]</sup> or hole transporting material in perovskite solar cells.<sup>[17,18]</sup> They were also applied in organic *n*-type,<sup>[19,20]</sup> *p*-type<sup>[21,22]</sup> or ambipolar<sup>[23]</sup> semiconductors build in organic field-effect transistors (OFET).

Over the last two decades, several reports on TT push-pull molecules **A** – **E** with nonlinear optical (NLO) properties appeared in the literature (Figure 1). Thieno[3,2-*b*]thiophene has been utilized as a central  $\pi$ -conjugated linker **A** equipped with chalcogen electron donors and formyl, nitro and tricyanovinyl acceptors. Second order polarizabilities 15 to  $43 \times 10^{-30}$  esu were measured by electric field-induced second harmonic generation (EFISH).<sup>[24]</sup> Andreu et al. have thoroughly investigated thieno[3,2-*b*]thiophene either as aromatic (**B**) or quinoid (**C**)  $\pi$ -linker in push-pull molecules with 4*H*-pyranilidene donor and dicyanovinyl, thiobarbituric acid or tricyanofuran acceptors. Whereas quinoid TT derivatives showed NLO responses ranging from 2100 to  $7900 \times 10^{-48}$  esu, the aromatic arrangement induces slightly lower nonlinearities with  $\mu\beta_0$  product between 650 and  $5100 \times 10^{-48}$  esu.<sup>[25]</sup> However, push-pull chromophores with tricyanofuran (TCF) or thiobarbiturate acceptors showed  $\mu\beta_0$  values ranging from 2800 to  $21900 \times 10^{-48}$  esu.<sup>[26]</sup> Raposo et al. have focused on 5-arylthieno[3,2-*b*]thiophene scaffold **D** and its utilization in construction of push-pull chromophores.<sup>[27]</sup> Variation of peripheral alkoxy/dialkylamino donors allowed tuning two-photon absorption (TPA) cross-section ( $\sigma_2$ ) within the range of 82 to 836 GM. In contrast to thieno[3,2-*b*]thiophene central  $\pi$ -linker, its isomers are much less investigated. One example shows thieno[2,3-*b*]thiophene incorporated into dithiacyclophane **E** with enhanced hyperpolarizability to  $21.6 \times 10^{-30}$  esu as measured by hyper-Rayleigh scattering (HRS).<sup>[4,28]</sup> From the aforementioned TT-derived NLOphores available in the literature, we can deduce:

- Thieno[3,2-*b*]thiophene is more investigated/popular than other TT regioisomers.
- TTs are mostly applied as a  $\pi$ -linker, not standalone donor.
- There is no systematic study distinguishing electronic behaviour of particular TT isomers.
- Also, there is no systematic study of the acceptor linked to TT.

Hence, the thesis reports herein a systematic study on two series of isomeric push-pull chromophores derived from thieno[3,2-*b*]thiophene and thieno[2,3-*b*]thiophene electron donors equipped with various electron-acceptor units at position 2 (Figure 1).

Fundamental properties of TT based compounds **1a – g** and **2a – g** were investigated by electrochemistry, UV-VIS absorption spectra, differential scanning calorimetry (DSC)/thermogravimetry (TGA) and nonlinear optical SHG/THG measurements. The experimental data is further completed and supported by DFT calculations.

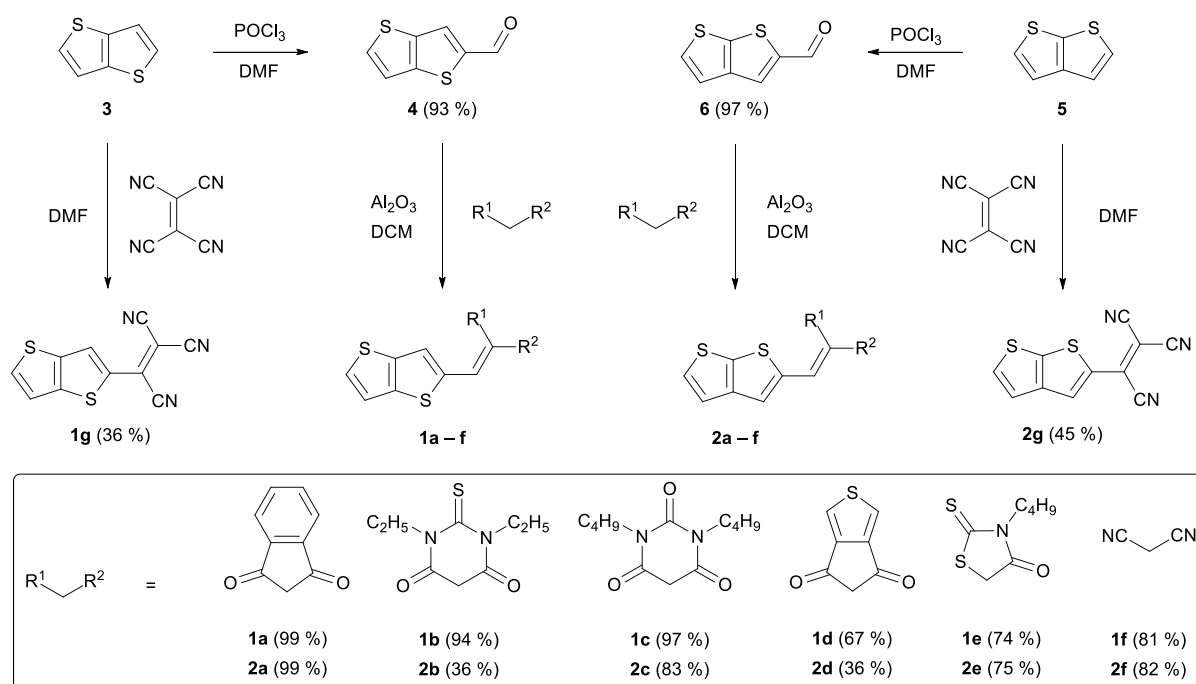


## 2. Aims of thesis

- The literature search elaboration focused on synthetic pathways, specific structural modifications and optoelectronic applications of the fused thiophene derivatives, specifically: thieno[3,2-*b*]thiophene, thieno[2,3-*b*]thiophene and 4*H*-cyclopenta[*c*]thiophen-4,6(5*H*)-dione
- Synthesis of the systematic series of target D- $\pi$ -A chromophores based on electron-donor thienothiophenes
- Structure and purity verification of all target compounds and intermediates using all available analytical methods
- Interpretation of structure-properties relationships for all target chromophores using all measured and calculated optoelectronic and thermal data

## 3. Results and discussion

### 3.1. Synthesis



**Scheme 1.** Overall synthetic route towards target TT chromophores **1a – g** and **2a – g**

Two series of push-pull chromophores **1a – g** and **2a – g** were synthesized as depicted on Scheme 1. The chromophores in series **1** were built on central thieno[3,2-*b*]thiophene **3**, whereas thieno[2,3-*b*]thiophene **5** represents leitmotiv in series **2**. The optimized synthesis of parent TT isomers **3** and **5** was realized according to methods listed in literature.<sup>[29–33]</sup> Target molecules **a – f** in both series were prepared via a two-step facile reaction sequence that utilizes Vilsmeier-Haack formylation and subsequent Knoevenagel condensation. Both aldehydes **4** and **6** were synthesised in high yields of 93 and 97 %, respectively. The Vilsmeier reagent had to be prepared separately by reacting phosphorus oxychloride and *N,N*-dimethylformamide (DMF) with subsequent dropwise addition to a solution of **3** or **5** in DMF. The final Knoevenagel condensation utilized three commercially available precursors - indan-1,3-dione (**a**), *N,N*-diethylthiobarbituric acid (**b**) and malononitrile (**f**); *N,N*-dibutylbarbituric acid (**c**),<sup>[34]</sup> ThDione (**d**)<sup>[35]</sup> and *N*-butylrhodanine (**e**)<sup>[36]</sup> were prepared according to literature. The final Knoevenagel reactions were carried out using aluminium oxide/DCM system at 25 °C<sup>[34]</sup> and provided the target chromophores in satisfactory yields 64 – 99 %, except for **2b** (36 %) and **2d** (36 %) that required repeated purification. The reaction with unsymmetrical *N*-butylrhodanine (**e**) afforded chromophores **1e** and **2e** as a mixture of *E/Z* isomers with the estimated ratio of 1:10 (based on <sup>1</sup>H NMR). Both series were completed by chromophores **1g** and **2g** bearing tricyanovinyl moiety that were introduced by reacting **3** or **5** with tetracyanoethylene (TCNE) in DMF.<sup>[37]</sup> These electrophilic substitution reactions provided **1g** and **2g** in 36 and 45 %, respectively. All attempts to react lithiated **3** or **5** (*n*BuLi or LDA) with TCNE did not improve the yields.

### 3.2. Thermal behaviour

Thermal properties and stability of compounds **1a–g** and **2a–g** were studied by differential scanning calorimetry (DSC) and thermogravimetric analysis (TGA). Melting points ( $T_m$ ) and temperatures of thermal decomposition ( $T_d$ ) were determined by DSC. Initial temperatures of thermal degradation ( $T_i$ ) and temperatures of 5% weight loss ( $T_5$ ) were determined by TGA. A representative thermogram of chromophore **2d** is shown on Figure 2 while  $T_m$ ,  $T_d$ ,  $T_i$  and  $T_5$  values for all chromophores are listed in Table 1.

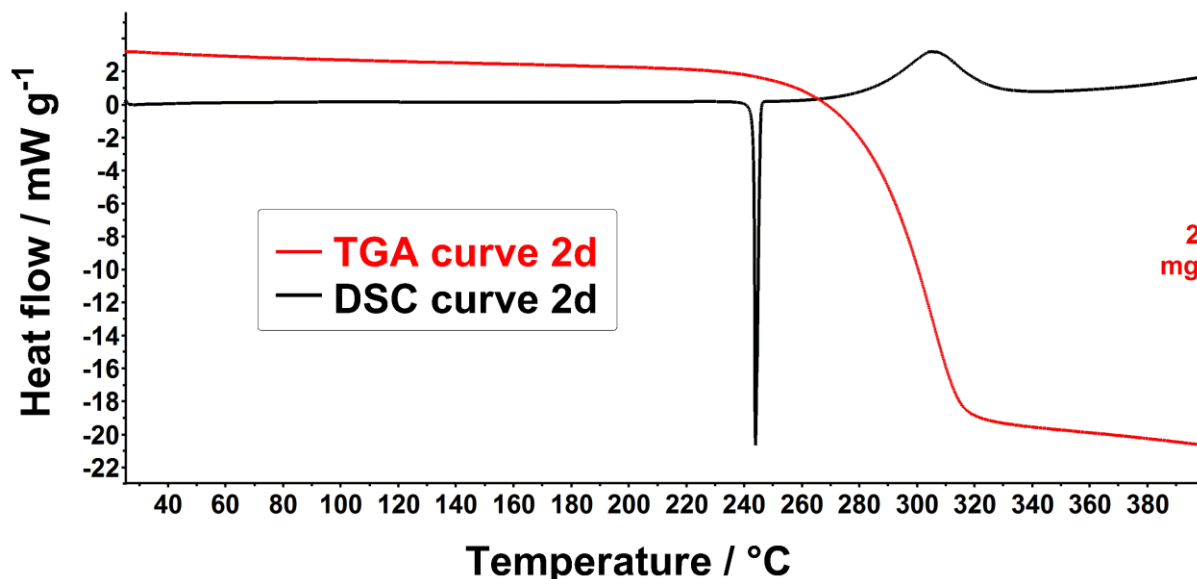


Figure 2. Representative DSC and TGA curves of compound **2d**

The parent unsubstituted TT isomers **3** ( $T_m = 56\text{ °C}$ )<sup>[38]</sup> and **5** ( $T_m = 6\text{ °C}$ )<sup>[2]</sup> differ significantly in their melting points by  $50\text{ °C}$ . However, the data gathered in Table 1 ( $T_m$  and  $T_d$ ) show that thermal properties of compounds **1a–g** and **2a–g** are rather influenced by the appended electron acceptor. When considering the DSC measurements, the following structure-property relationships can be deduced:

- The highest melting points were recorded for **1d/2d** and **1g/2g** derivatives bearing ThDione or tricyanovinyl substituents (e.g. **1d/1g** with  $T_m = 239/241\text{ °C}$ ).
- An introduction of *N*-butyl chains lowers melting points by approximately  $65\text{ °C}$  (e.g. **2b/2c** with  $T_m = 216/150\text{ °C}$ ).
- TTs bearing *N*-butylrhodanine or malononitrile moieties proved the highest thermal robustness in liquid phase (e.g. **2e/2f** with  $T_d = 340/345\text{ °C}$ ).
- *N,N*-Diethylthiobarbiturate-substituted compounds **1b** and **2b** showed the lowest  $T_d$  value of  $250\text{ °C}$ .
- TTs **1e** and **2e** with *N*-butylrhodanine showed relatively early melting, postponed decomposition and thus resulting largest difference between  $T_m$  and  $T_d$  values ( $142\text{ °C}$  and  $178\text{ °C}$  respectively).

According to DSC results, TGA did reveal impact of TT isomer used. An average difference in  $T_i$  values of the given pair of isomers is approximately  $7\text{ °C}$ . The following general trends can be deduced from the measured TGA data:

- ThDione derivatives **1d** and **2d** possess the highest thermal stability ( $T_i = 229$  °C and  $236$  °C, respectively).
- Cyano-substituted derivatives showed the lowest  $T_i$  values ( $180/168$  °C for **1f/2f** and  $196/184$  °C **1g/2g**).
- Compared to DSC ( $T_m$ ), the influence of *N*-butyl chains is less evident from TGA data ( $T_i$ ). However, compounds **c** and **e** showed  $T_i$  significantly higher than  $T_m$ , which indicates their thermally stable and non-volatile liquid phase (e.g. **1c** with  $T_i = 226$  °C and  $T_m = 160$  °C).
- On the contrary, cyano-substituted compounds **f** and **g** decomposed prior to melting (e.g. **1f** with  $T_i = 180$  °C and  $T_m = 226$  °C). This holds true even for **1g** and **2g** with one of the highest melting points across both series.

### 3.3. Electrochemistry

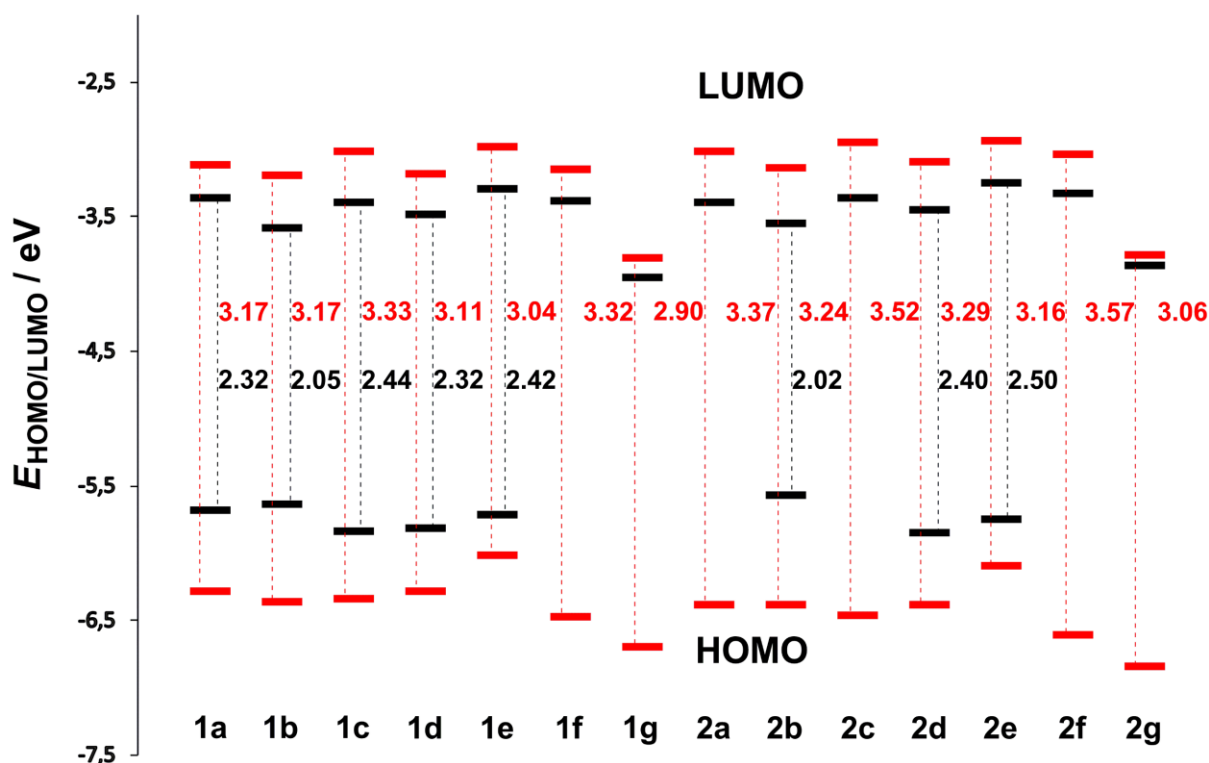


**Figure 3.** Energy level diagram of the electrochemical (black) and DFT (red) derived energies of the  $E_{HOMO/LUMO}$  for chromophores **1a – g** and **2a – g**

The electrochemical behaviour of target chromophores **1a – g** and **2a – g** was investigated by cyclic voltammetry (CV) in DMF. All target compounds showed irreversible reductions except for **1g** and **2g** whose reduction processes are reversible. The oxidation of **1a – e**, **2b**, **2d** and **2e** is represented by irreversible process. The half-wave potentials of the first oxidation ( $E_{1/2(ox1)}$ ) for chromophores **1f**, **1g**, **2a**, **2c**, **2f** and **2g** were not determined due to localization of their oxidation process out of DMF potential window. The measured half-wave potentials of the first oxidation ( $E_{1/2(ox1)}$ ) and reduction ( $E_{1/2(red1)}$ ) as well as the corresponding HOMO ( $E_{HOMO}$ ), LUMO ( $E_{LUMO}$ ) energies<sup>[39]</sup> and their differences ( $\Delta E$ ) are listed in Table 1 and visualized in the energy level diagram shown in Figure 3 jointly with the DFT calculated values. The  $E_{HOMO}$  ranges from  $-5.58$  to  $-5.86$  eV, while  $E_{LUMO}$  from  $-3.26$  to  $-3.96$  eV. The  $\Delta E$  values are

within the range of 2.02 to 2.50 eV. Based on the measured electrochemical data, the following conclusions can be made.

- The particular chromophores in both series **1** and **2** obey the same trend (see Figure 3).
- With diminished alternation of  $E_{\text{HOMO}}$  values (as compared for available values for **1b/2b**, **1d/2d** and **1e/2e**), the principal changes are seen on the LUMO level.
- The LUMO is slightly more negative/deepened for chromophores built on thieno[3,2-*b*]thiophene (except for **1a/2a**).
- The average HOMO-LUMO differences between both series **1** and **2** are below 0.1 V. Hence, the used TT isomer affects the electrochemical behaviour of the resulting chromophore negligibly.

According to increasing  $\Delta E$  (only limited electrochemical data available), the chromophores in series **1** can roughly be ordered as **b** > **a**  $\geq$  **d** > **e** > **c**. This order obey decreasing electron withdrawing efficiency of the appended acceptors.<sup>[34]</sup>

**Table 1.** Thermal, electrochemical and DFT calculated data for chromophores **1a – g** and **2a – g**

Compound	$T_m$ [°C] <sup>a</sup>	$T_d$ [°C] <sup>a</sup>	$T_i$ [°C] <sup>b</sup>	$T_5$ [°C] <sup>b</sup>	$E_{1/2(\text{ox1})}$ [V] <sup>c</sup>	$E_{1/2(\text{red1})}$ [V] <sup>c</sup>	$E_{\text{HOMO}}$ [eV] <sup>d</sup>	$E_{\text{LUMO}}$ [eV] <sup>d</sup>	$\Delta E$ [eV]	$E_{\text{HOMO}}^{\text{DFT}}$ [eV] <sup>e</sup>	$E_{\text{LUMO}}^{\text{DFT}}$ [eV] <sup>e</sup>	$\Delta E^{\text{DFT}}$ [eV]	$\mu$ [D] <sup>e</sup>
<b>1a</b>	226	300	213	254	1.30	-1.02	-5.69	-3.37	2.32	-6.29	-3.12	3.17	2.9
<b>1b</b>	226	250	218	248	1.26	-0.79	-5.65	-3.60	2.05	-6.37	-3.20	3.17	7.9
<b>1c</b>	160	290	226	254	1.46	-0.98	-5.85	-3.41	2.44	-6.35	-3.02	3.33	5.8
<b>1d</b>	239	280	229	266	1.43	-0.89	-5.82	-3.50	2.32	-6.29	-3.19	3.10	3.1
<b>1e</b>	178	320	217	253	1.33	-1.09	-5.72	-3.30	2.42	-6.02	-2.99	3.03	6.7
<b>1f</b>	226	- <sup>f</sup>	180	206	- <sup>g</sup>	-0.99	-	-3.40	-	-6.48	-3.16	3.32	11.1
<b>1g</b>	241	305	196	219	- <sup>g</sup>	-0.43	-	-3.96	-	-6.70	-3.81	2.89	12.7
<b>2a</b>	233	295	215	255	- <sup>g</sup>	-0.98	-	-3.41	-	-6.39	-3.02	3.37	2.1
<b>2b</b>	216	250	223	247	1.19	-0.83	-5.58	-3.56	2.02	-6.39	-3.15	3.24	7.7
<b>2c</b>	150	285	214	248	- <sup>g</sup>	-1.02	-	-3.37	-	-6.47	-2.96	3.51	5.6
<b>2d</b>	243	280	236	268	1.47	-0.93	-5.86	-3.46	2.40	-6.39	-3.10	3.29	2.3
<b>2e</b>	162	340	217	255	1.37	-1.13	-5.76	-3.26	2.50	-6.10	-2.94	3.16	7.1
<b>2f</b>	192	345	168	197	- <sup>g</sup>	-1.05	-	-3.34	-	-6.61	-3.04	3.57	11.6
<b>2g</b>	230	270	184	211	- <sup>g</sup>	-0.52	-	-3.87	-	-6.85	-3.79	3.06	12.1

<sup>a</sup>Determined by DSC in open aluminous crucibles under N<sub>2</sub> inert atmosphere and with a scanning rate of 3 °C/min within the range of 25 – 400 °C. Melting point and temperature of decomposition were determined as intersection of the baseline and tangent of the peak (onset point). <sup>b</sup>Determined by TGA in open alumina crucibles under N<sub>2</sub> inert atmosphere and with a heating rate of 3 °C/min within the range of 25 – 400 °C. The initial temperature of degradation was determined as the last common point of TGA curve and its first derivation (DTG curve). Temperature of 5% weight loss was determined by gradual horizontal step on TGA curve. <sup>c</sup> $E_{1/2(\text{ox1})}$  and  $E_{1/2(\text{red1})}$  are half-wave potentials of the first oxidation and reduction measured in DMF; all potentials are given vs SSCE. <sup>d</sup>Recalculated from the  $E_{1/2(\text{ox1/red1})}$  according to the equation  $-E_{\text{HOMO/LUMO}} = E_{1/2(\text{ox1/red1})} + 4.35 + 0.036$ .<sup>34</sup> <sup>e</sup>Calculated at the DFT B3LYP/6-311++G(2df,p) level in DMF. <sup>f</sup>Evaporated at 350°C. <sup>g</sup>The oxidation processes are localized out of the available potential window in DMF.

### 3.4. Linear optical properties

Fundamental optical properties of target chromophores were investigated by electronic absorption spectra measured in DMF at concentration of  $1 \times 10^{-5}$  M. Spectra of chromophores in series **1/2** are shown in Figure 4/Figure 5 as a dependence of the molar extinction coefficient ( $\epsilon$ ) on the wavelength ( $\lambda$ ). Table 2 summarizes the measured longest-wavelength absorption maxima ( $\lambda_{\text{max}}^{\text{A}}$ ) and corresponding molar extinction coefficients ( $\epsilon$ ). The main feature of the spectra is presence of a single band located within the spectral range of 375 to 475 nm. The spectra shown in Figure 6 compares chromophores **1d** and **2d** that differ in the used TT isomer (both ThDione acceptor). It is obvious that the spectrum of **1d** is slightly bathochromically shifted,

which holds true for all pairs of chromophores. The average difference  $\Delta\lambda_{\max}^A$  is 10 nm. This implies slightly higher electron releasing ability of thieno[3,2-*b*]thiophene (series **1**) over thieno[2,3-*b*]thiophene (series **2**). This observation is consistent with the aforementioned electrochemical measurements.

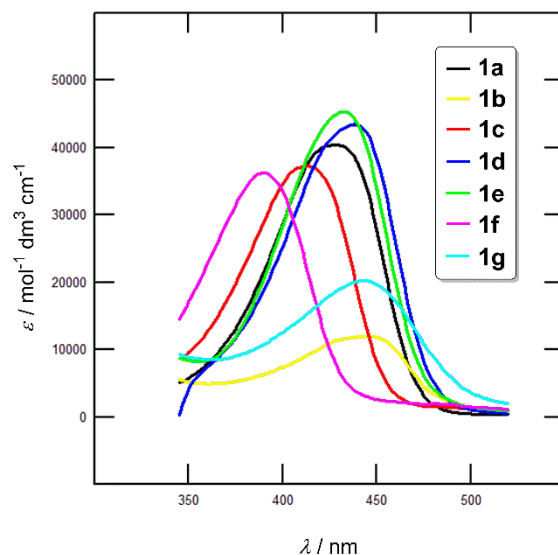
**Table 2.** Optical properties of chromophores **1a – g** and **2a – g**

Com.	$\lambda_{\max}^A$ [nm (eV)] <sup>a</sup>	$\epsilon$ [ $\times 10^3 \text{ M}^{-1}\text{cm}^{-1}$ ] <sup>a</sup>	$\lambda_{\max}^{\text{TD-DFT}}$ [nm (eV)] <sup>b</sup>	$\lambda_{\max}^{\text{ZINDO}}$ [nm(eV)] <sup>b</sup>	SHG [ $\text{pm}\cdot\text{V}^{-1}$ ] <sup>c</sup>	PISHG [ $\text{pm}\cdot\text{V}^{-1}$ ] <sup>d</sup>	THG [a.u.] <sup>e</sup>	$\beta$ [ $\times 10^{-30} \text{ esu}$ ] <sup>f</sup>	$\gamma$ [ $\times 10^{-25} \text{ esu}$ ] <sup>g</sup>
<b>1a</b>	433 (2.86)	40.5	405 (3.06)	453 (2.74)	1.71	2.01	7.97	76.8	2.06
<b>1b</b>	446 (2.78)	12.2	405 (3.06)	468 (2.65)	1.31	1.82	8.22	17.7	16.13
<b>1c</b>	414 (3.00)	37.5	368 (3.37)	459 (2.70)	0.71	1.02	1.59	33.1	17.51
<b>1d</b>	441 (2.81)	43.9	415 (2.99)	459 (2.70)	2.45	2.61	4.09	10.4	1.52
<b>1e</b>	434 (2.86)	46.0	413 (3.00)	431 (2.88)	0.78	1.12	7.40	58.0	0.98
<b>1f</b>	389 (3.19)	36.8	353 (3.51)	446 (2.78)	0.80	1.32	7.40	25.1	0.11
<b>1g</b>	445 (2.79)	20.5	398 (3.12)	467 (2.66)	1.80	2.28	7.45	57.4	0.09
<b>2a</b>	413 (3.00)	40.1	382 (3.25)	415 (2.99)	2.03	2.31	2.44	66.1	2.27
<b>2b</b>	444 (2.79)	16.4	390 (3.18)	436 (2.84)	1.35	1.83	7.30	21.4	11.33
<b>2c</b>	406 (3.05)	29.2	365 (3.40)	426 (2.91)	0.62	0.92	1.67	31.3	12.91
<b>2d</b>	430 (2.88)	37.6	392 (3.16)	422 (2.94)	2.38	2.55	3.40	88.1	1.35
<b>2e</b>	423 (2.93)	57.0	402 (3.08)	396 (3.13)	0.80	1.31	5.60	55.6	0.90
<b>2f</b>	383 (3.24)	28.6	350 (3.54)	408 (3.04)	0.76	1.35	5.60	22.2	0.03
<b>2g</b>	430 (2.88)	23.9	394 (3.15)	435 (2.85)	1.70	2.22	5.60	48.1	0.03

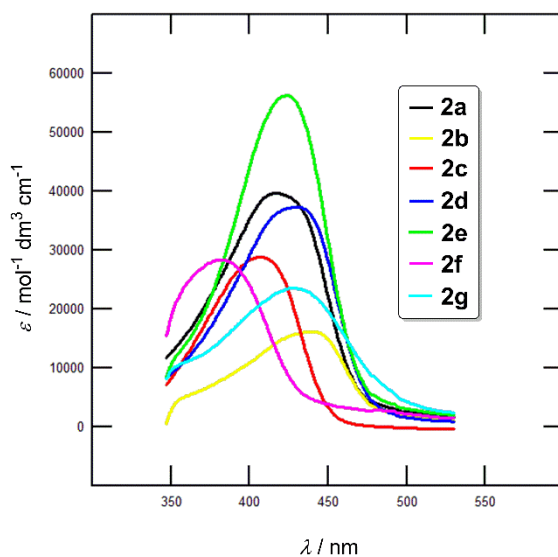
<sup>a</sup>Measured in *N,N*-dimethylformamide at concentration of  $1 \times 10^{-5} \text{ M}$ . <sup>b</sup>Calculated at the DFT B3LYP/6-311++G(2df,p) level in vacuum <sup>c</sup>Measured with a 1064 nm source fundamental laser beam. <sup>d</sup>Photoinduced SHG. <sup>e</sup>Measured with a 1540 nm source fundamental laser beam. <sup>f</sup>Calculated at the DFT B3LYP/6-311++G(2df,p) level in vacuum at 1064 nm. <sup>g</sup>Calculated by using the PM7 semi-empirical method implemented in MOPAC.

Figure 4 and 5 shows absorption spectra of all chromophores in series **1** and **2**, respectively. Whereas the longest-wavelength absorption maxima were found within a spectral range of 383 – 446 nm, the corresponding extinction coefficients range from 12 to  $57 \times 10^3 \text{ M}^{-1}\text{cm}^{-1}$ . Thus, the optical gap of TT push-pull molecules **1** and **2** can be tuned within a range of 3.24 – 2.78 eV by attaching various electron withdrawing moieties. The chromophores can be arranged in the following order according to their increasing optical gap: **b** > **g**  $\geq$  **d** > **e** > **a** > **c** > **f**. This trend further extends the electrochemical outcomes and obeys the electron withdrawing efficiency of the appended acceptors (*N,N*-diethylthiobarbiturate > tricyanovinyl > ThDione > *N*-butylrhodanine > indan-1,3-dione > *N,N*-dibutylbarbiturate > dicyanovinyl).<sup>[34]</sup> As can be seen, simple O→S chalcogen replacement as in barbituric (**c**) and thiobarbituric acid (**b**) brings considerable bathochromic shift [compare also Thdione (**d**) and analogous indan-1,3-dione (**a**)]. Increasing number of cyano groups has similar effect, e.g. tricyanovinyl (**g**) and dicyanovinyl (**f**). Five-membered rhodanine (**e**) proved to be average electron acceptor among the investigated series.

Chromophores also considerably differ in their extinction coefficients. Chromophores featuring the acceptors with the most extended  $\pi$ -system (**d** and **a**) as well as rhodanine (**e**) showed the highest  $\epsilon$  values. On the contrary, chromophores with the strongest acceptor, thiobarbituric acid (**b**) and tricyanovinyl (**g**), possess two- to three-times lower extinction coefficients.



**Figure 4.** UV-VIS absorption spectra of chromophores **1a** – **g** measured in DMF at  $c = 1 \times 10^{-5}$  M



**Figure 5.** UV-VIS absorption spectra of chromophores **2a** – **g** measured in DMF at  $c = 1 \times 10^{-5}$  M

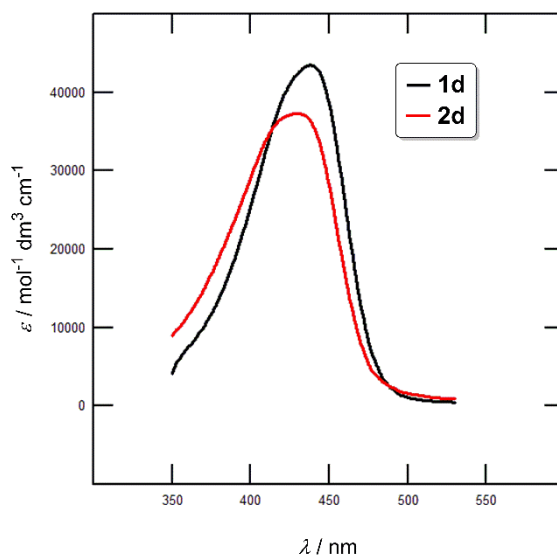


**Figure 6.** Comparison of absorption spectra between isomers **1d** and **2d** measured in DMF at  $c = 1 \times 10^{-5}$  M

### 3.5. Nonlinear optical properties

Due to their prospective application as high-speed communication modulators,<sup>[40]</sup> a significant effort is currently devoted to small organic molecules with NLO activity,<sup>[41]</sup> especially those with donor/ $\pi$ -linker doped with various heteroatoms.<sup>[42]</sup> Hence, beside linear optical properties, optical nonlinearities of TTs **1** and **2** have been also investigated, second- and third-harmonic generations (SHG and THG) in particular. The SHG and THG measurements were carried out with 1064 nm Nd:YAG (SHG) and 1540 nm (THG) Er:glass fundamental laser beams. The application of the 1540 nm was caused by a necessity to avoid fundamental absorption at the third harmonic wavelength (about 513 nm). The frequency repetition of the beam pulses was varied within 10 to 30 Hz. The photothermal control has shown that the changes of temperature did not exceed 2 – 3 K. The set of filters at doubled (532 nm) and tripled frequency (513 nm) have been applied to spectrally separate the third order nonlinear optical signal from the first order. Samples with known parameter of the nonlinear optical susceptibilities have been used as reference specimens. The studied chromophores have been embedded into oligoetheracrylate photopolymer matrices and were additionally poled by dc-electric field similarly as described in literature.<sup>[43]</sup>

The principal results of the NLO measurements are given in Table 2. The experimental second-order polarizabilities (SHG) range from 0.62 to 2.45  $\text{pm}\cdot\text{V}^{-1}$  and are clearly function of the appended acceptor. The measured SHG nonlinearities are very close to the recently obtained parameters of second order susceptibilities for substituted 1,3,5-triphenylpyrazolines measured by the same set-up (1.67 – 2.7  $\text{pm}\cdot\text{V}^{-1}$ ).<sup>[44]</sup> The effect of the used TT isomer is less pronounced. The highest SHG responses have been observed for chromophores **1d** and **2d** (2.45 and 2.38  $\text{pm}\cdot\text{V}^{-1}$ ) with ThDione acceptor followed by their structural analogues **1a** and **2a** (1.71 and 2.03  $\text{pm}\cdot\text{V}^{-1}$ ) with indan-1,3-dione. Noticeable nonlinearities were also recorded for tricyanovinyl-terminated TTs **1g** and **2g** (1.80 and 1.70  $\text{pm}\cdot\text{V}^{-1}$ ). Chromophores **1b** and **2b** with *N,N*-diethylthiobarbiturate residues afforded SHG nonlinearities of 1.31 and 1.35  $\text{pm}\cdot\text{V}^{-1}$ . Thus, the highest SHG responses were measured for chromophores with either strong electron acceptors (**d**, **g**, **b**) or with extended  $\pi$ -system (**a**).



Chromophores bearing *N,N*-dibutylbarbiturate (**c**), *N*-butylrhodanine (**e**) and dicyanovinyl (**f**) proved less efficient SHG materials. Photoinduced SHG (PISHG) showed the same trends with the highest nonlinearities recorded for chromophores **d**, **a** and **g**. However, the PISHG was principally more stable than that measured for tetranuclear copper  $\pi$ -complexes with thiazolidinone ligands.<sup>[45]</sup> So, TTs **1** and **2** seem to be well-suited organic materials for tuning SHG as their responses are completely reversible after interrupting the process and no changes in the SHG were encountered.

Third-order NLO activity of TTs **1** and **2** has been examined by THG. Considering the data gathered in Table 2, it is obvious that chromophores **1c** and **2c** end-capped with *N,N*-dibutylbarbiturate acceptors possess very weak third nonlinearities (1.59 and 1.67 a.u.). This is in contrast to chromophores **1b** and **2b** with *N,N*-diethylthiobarbiturate that have shown the largest THG responses 8.22 and 7.30 a.u. This again implies that O $\rightarrow$ S chalcogen replacement plays very important role. On the contrary, replacement of fused benzene ring as in indan-1,3-dione derivatives **1a** by thiophene in **1d** has detrimental effect on third order NLO activity. However, this is in contrast to opposite TT isomer **2a** vs. **2d**. Rhodanine, di- and tricyanovinyl-terminated chromophores **e**, **f** and **g** showed very similar THG values around 7.40 and 5.60 a.u. for TT isomers **1** and **2**, respectively. Compared to aforementioned 1,3,5-triphenylpyrazolines and copper  $\pi$ -complexes with thiazolidinone ligands, the measured THG responses of TTs **1** and **2** are slightly lower.

### 3.6. DFT calculations

Spatial and electronic properties of all target chromophores **1a – g** and **2a – g** were investigated at the DFT level by using the Gaussian<sup>®</sup> 16 software package.<sup>[46]</sup> The geometries of molecules **1a – g** and **2a – g** were optimized using DFT B3LYP/6-311G(2df,p) method. Energies of the HOMO and the LUMO, their differences and ground-state dipole moments  $\mu$  were calculated on the DFT B3LYP/6-311++G(2df,p) level including DMF as a solvent (Table 1). First hyperpolarizabilities  $\beta$  were calculated on the DFT B3LYP/6-311++G(2df,p) level in vacuum at 1064 nm. Second hyperpolarizabilities  $\gamma$  were calculated by PM7 semi-empirical method implemented in MOPAC<sup>[47]</sup> using DFT-optimized geometries (Table 2). The electronic absorption spectra, longest-wavelength absorption maxima and corresponding electron transitions were calculated using TD-DFT and ZINDO (nstates = 8) B3LYP/6-311++G(2df,p) (Table 2). The calculated HOMO/LUMO energies of **1a – g** and **2a – g** are within the range of  $-6.85$  to  $-6.02$  eV and  $-3.81$  to  $-2.94$  eV, respectively (Table 1). As can be seen from the energy level diagram shown in Figure 3, the DFT-calculated  $E_{\text{HOMO}}/E_{\text{LUMO}}$  are slightly under- an overestimated as compared to the electrochemical values. However, the used DFT method is clearly capable to describe trends within both series and, therefore, it can be considered as a reasonable tool for describing electronic and spatial properties of TTs **1** and **2**. A tight correlation has been found between complete experimental and DFT-calculated  $E_{\text{LUMO}}$  values. By comparing corresponding pairs of chromophores,

the LUMO energies of **1** with thieno[3,2-*b*]thiophene is slightly lower, similarly as found by electrochemistry.

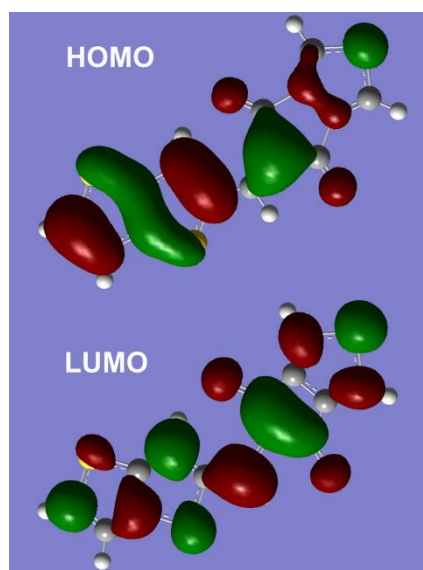


Figure 7. HOMO and LUMO localizations in **1d**

The HOMO and LUMO localizations in representative chromophore **1d** are shown in Figure 7. The HOMO is predominantly localized on the TT donor and partially also in alternating position of the appended double bond. The LUMO is mostly spread over the appended acceptor, partially also over the TT's  $\pi$ -conjugated system. Both HOMO and LUMO are partially separated which further confirms CT character of chromophores **1** and **2**. Derivatives **1b** and **2b** bearing thiobarbituric acid pendant possess the HOMO localized on the sulphur atom of the thiobarbiturate, the LUMO is spread over the whole  $\pi$ -system. This is in agreement to our recent observation<sup>[34]</sup> and also corresponds to localization of frontier orbitals reported by Khurana et al. for thiobarbiturates with none mezoeric donor.<sup>[48]</sup>

The calculated ground-state dipole moments range from 2.1 to 12.7 D (Table 1) and are clearly function of the structure/symmetry. For instance, chromophores **f** and **g** bearing dicyanovinyl and tricyanovinyl groups possess the highest values of  $\mu$  (11.1 – 12.7 D). On the contrary, the lowest dipole moments of 2.1 – 3.1 D were found for structural analogues **a** and **d** bearing indan-1,3-dione and ThDione.

Electronic absorption spectra of TTs **1** and **2** calculated by TD-DFT revealed one single band appearing within the range of 350 to 415 nm. Compared to experimental  $\lambda_{\max}^A$  values are the calculated maxima  $\lambda_{\max}^{\text{TD-DFT}}$  hypsochromically shifted. However, both quantities showed tight correlation. Chromophores in series **1** showed slightly red-shifted  $\lambda_{\max}^{\text{TD-DFT}}$  values, which further confirms higher electron releasing ability of thieno[3,2-*b*]thiophene. TD-DFT calculation is also capable to identify chromophores with the weakest acceptors such as **c** and **f** but there is no clear trend in the remaining groups. However, ZINDO calculations confirmed the most bathochromically shifted maxima for chromophores **b**, **d** and **g**. The observed single band of the spectra is mostly generated by HOMO $\rightarrow$ LUMO and HOMO(-1) $\rightarrow$ LUMO transitions

The calculated NLO coefficients  $\beta$  and  $\gamma$  range from 10.4 to  $76.8 \times 10^{-30}$  esu and from 0.03 to  $17.51 \times 10^{-25}$  esu, respectively. The highest  $\beta$  coefficients were calculated for **a** and **d** chromophores, similarly to SHG (taking value for **1d** as an outlier). For chromophores **g** and **e** with tricyanovinyl and rhodanine acceptors were also calculated noticeable nonlinearities. Semi-empirical PM7 calculation of  $\gamma$  identified chromophores **b** and **c** bearing (thio)barbiturate acceptors as the most active. This is in agreement with experiment that revealed thiobarbiturate derivatives **1b** and **2b** as most active THG materials. However, the results calculated for barbiturate derivatives **1c** and **2c** is in a complete contradiction.

## 4. Conclusion

In conclusion, we have designed small D- $\pi$ -A chromophores utilizing thieno[3,2-*b*]thiophene and thieno[2,3-*b*]thiophene as electron donors. Fourteen new chromophores in two series were conveniently prepared via Vilsmeier-Haack formylation and Knoevenagel condensation or substitution. The fundamental optoelectronic properties were tuned by varying both donor and acceptor. The observed structure-property relationships within the investigated series of thienothiophenes **1** and **2** can be generalized as follows (Figure 8):

- Despite the parent TT isomers differ considerably in melting points, thermal properties of push-pull derivatives **1** and **2** are mostly affected by the appended acceptor. Novel ThDione acceptor proved thermally very stable, whereas alkyl chains of (thio)barbiturate and rhodanine acceptors bring considerably lowered melting points but improved thermal robustness in liquid phase.
- Electrochemical measurements of TTs **1** and **2** revealed slightly improved electron donating ability of thieno[3,2-*b*]thiophene.
- Linear optical properties measured by electronic absorption spectra indicated bathochromically shifted longest-wavelength absorption maxima of TT **1** bearing thieno[3,2-*b*]thiophene.
- Molar extinction coefficients of chromophores **1** and **2** primarily depend on the  $\pi$ -system extension.
- The used acceptor also strongly affects the nonlinear optical properties.
- Based on the aforementioned observations, we can order electron withdrawing efficiency of the particular acceptors: *N,N*-diethylthiobarbiturate > tricyanovinyl > ThDione > *N*-butylrhodanine > indan-1,3-dione > *N,N*-dibutylbarbiturate > dicyanovinyl.
- As a general conclusion, appended acceptor seems to have larger influence on the fundamental optoelectronic/thermal properties of **1** and **2** than parent TT isomer.
- Thieno[3,2-*b*]thiophene-derived push-pull molecules **1d** and **1b** bearing either polarizable ThDione or strong thiobarbiturate acceptors proved to be most efficient second- and third-order NLOphores.

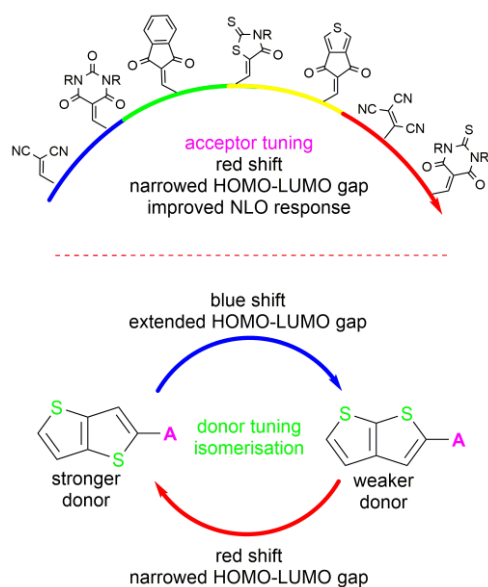


**Figure 8.** Principal property tuning of TT derivatives **1** and **2** achieved in this work

In view of the current interest in functionalized organic conjugated molecules, I believe that the aforementioned structure-property relationships would serve as a guide in designing new molecules with tailored properties.

## 5. List of References

- [1] I. F. Perepichka, D. F. Perepichka, V knize: *Handbook of Thiophene-Based Materials: Applications in Organic Electronics and Photonics*, John Wiley And Sons, **2009**.
- [2] F. Challenger, J. B. Harrison, *J. Inst. Pet. Technol.* **1935**, *21*, 135–147.
- [3] A. Biedermann, P. Jacobson, *Chem. Ber.* **1886**, *19*, 2444–2447.
- [4] S. H. Mashraqui, S. Ghadigaonkar, M. Ashraf, A. Sri Ranjini, S. Ghosh, P. K. Das, *Tetrahedron* **2007**, *63*, 10011–10017.
- [5] I. Meager, R. S. Ashraf, S. Rossbauer, H. Bronstein, J. E. Donaghey, J. Marshall, B. C. Schroeder, M. Heeney, T. D. Anthopoulos, I. McCulloch, *Macromolecules* **2013**, *46*, 5961–5967.
- [6] T. Inouchi, T. Nakashima, T. Kawai, *Chem. - Asian J.* **2014**, *9*, 2542–2547.
- [7] A. Zhang, H. Xiao, S. Cong, M. Zhang, H. Zhang, S. Bo, Q. Wang, Z. Zhen, X. Liu, *J. Mater. Chem. C* **2015**, *3*, 370–381.
- [8] S. S. M. Fernandes, M. C. R. Castro, I. Mesquita, L. Andrade, A. Mendes, M. M. M. Raposo, *Dyes Pigm.* **2017**, *136*, 46–53.
- [9] J. K. Lee, S. Lee, S. J. Yun, *Bull. Korean Chem. Soc.* **2013**, *34*, 2148–2154.
- [10] J. Kulhánek, F. Bureš, J. Opršal, W. Kuznik, T. Mikysek, A. Růžička, *Asian J. Org. Chem.* **2013**, *2*, 422–431.
- [11] W. Tang, T. Lin, L. Ke, Z.-K. Chen, *J. Polym. Sci., Part A: Polym. Chem.* **2008**, *46*, 7725–7738.
- [12] E. N. Rodlovskaya, V. A. Vasnev, A. V Naumkin, A. A. Vashchenko, D. O. Goriachiy, *High Perform. Polym.* **2017**, *29*, 704–707.
- [13] Q. Zhang, Y. Wang, B. Kan, X. Wan, F. Liu, W. Ni, H. Feng, T. P. Russell, Y. Chen, *Chem. Commun.* **2015**, *51*, 15268–15271.
- [14] V. Tamilavan, S. Kim, J. Sung, D. Y. Lee, S. Cho, Y. Jin, J. Jeong, S. H. Park, M. H. Hyun, *Org. Electron. Phys. Mater. Appl.* **2017**, *42*, 34–41.
- [15] H. S. Lee, J. S. Lee, A. R. Jung, W. Cha, H. Kim, H. J. Son, J. H. Cho, B. S. Kim, *Polymer* **2016**, *105*, 79–87.
- [16] S. Zhu, Z. An, X. Chen, P. Chen, Q. Liu, *Dyes Pigm.* **2015**, *116*, 146–154.
- [17] X. Liu, F. Kong, F. Guo, T. Cheng, W. Chen, T. Yu, J. Chen, Z. Tan, S. Dai, *Dyes Pigm.* **2017**, *139*, 129–135.
- [18] S.-H. Peng, T.-W. Huang, G. Gollavelli, C.-S. Hsu, *J. Mater. Chem. C* **2017**, *5*, 5193–5198.
- [19] M. Durso, D. Gentili, C. Bettini, A. Zanelli, M. Cavallini, F. De Angelis, M. Grazia Lobello, V. Biondo, M. Muccini, R. Capelli, et al., *Chem. Commun.* **2013**,

49, 4298–4300.

- [20] Y. Shu, A. Mikosch, K. N. Winzenberg, P. Kemppinen, C. D. Easton, A. Bilic, C. M. Forsyth, C. J. Dunn, T. B. Singh, G. E. Collis, *J. Mater. Chem. C* **2014**, *2*, 3895–3899.
- [21] Z. Fei, P. Pattanasattayavong, Y. Han, B. C. Schroeder, F. Yan, R. J. Kline, T. D. Anthopoulos, M. Heeney, *J. Am. Chem. Soc.* **2014**, *136*, 15154–15157.
- [22] J. Yue, S. Sun, J. Liang, W. Zhong, L. Lan, L. Ying, F. Huang, W. Yang, Y. Cao, *J. Mater. Chem. C* **2016**, *4*, 2470–2479.
- [23] S. Mu, K. Oniwa, T. Jin, N. Asao, M. Yamashita, S. Takaishi, *Org. Electron. Phys. Mater. Appl.* **2016**, *34*, 23–27.
- [24] M. Blenkle, P. Boldt, C. Bräuchle, W. Grahn, I. Ledoux, H. Nerenz, S. Stadler, J. Wichern, J. Zyss, *J. Chem. Soc., Perkin Trans. 2* **1996**, 1377–1384.
- [25] A. B. Marco, R. Andreu, S. Franco, J. Garín, J. Orduna, B. Villacampa, B. E. Diosdado, J. T. López Navarrete, J. Casado, *Org. Biomol. Chem.* **2013**, *11*, 6338–6349.
- [26] A. B. Marco, R. Andreu, S. Franco, J. Garín, J. Orduna, B. Villacampa, R. Alicante, *Tetrahedron* **2013**, *69*, 3919–3926.
- [27] M. M. M. Raposo, C. Herbivo, V. Hugues, G. Clermont, M. C. R. Castro, A. Comel, M. Blanchard-Desce, *Eur. J. Org. Chem.* **2016**, 5263–5273.
- [28] S. H. Mashraqui, Y. S. Sangvikar, A. Meetsma, *Tetrahedron Lett.* **2006**, *47*, 5599–5602.
- [29] Y. H. Song, B. S. Jo, *J. Heterocycl. Chem.* **2009**, *46*, 1132–1136.
- [30] L. S. Fuller, B. Iddon, K. a Smith, *J. Chem. Soc., Perkin Trans.* **1997**, *1*, 3465–3470.
- [31] G. Cahiez, A. Moyeux, O. Gager, M. Poizat, *Adv. Synth. Catal.* **2013**, *355*, 790–796.
- [32] Affinium Pharmaceuticals Inc., Patent: *EP1226138 B1*, **2004**.
- [33] J. D. Prugh, G. D. Hartman, P. J. Mallorga, B. M. Mckeever, S. R. Michelson, M. A. Murcko, H. Schwam, R. L. Smith, J. M. Sondey, J. P. Springer, et al., *J. Med. Chem.* **1991**, 1805–1818.
- [34] M. Klikar, V. Jelínková, Z. Růžicková, T. Mikysek, O. Pytela, M. Ludwig, F. Bureš, *Eur. J. Org. Chem.* **2017**, 2764–2779.
- [35] P. Solanke, S. Achelle, N. Cabon, O. Pytela, A. Barsella, B. Caro, F. Robin-le Guen, J. Podlesný, M. Klikar, F. Bureš, *Dyes Pigm.* **2016**, *134*, 129–138.
- [36] M. R. Busireddy, V. N. R. Mantena, N. R. Chereddy, B. Shanigaram, B. Kotamarthi, S. Biswas, G. D. Sharma, J. R. Vaidya, *Org. Electron.* **2016**, *37*, 312–325.

- [37] K. Ogura, R. Zhao, T. Mizuoka, M. Akazome, S. Matsumoto, *Org. Biomol. Chem.* **2003**, *1*, 3845–3850.
- [38] K. B. Landenberger, A. J. Matzger, *Cryst. Growth Des.* **2012**, *12*, 3603–3609.
- [39] A. A. Isse, A. Gennaro, *J. Phys. Chem. B* **2010**, *114*, 7894–7899.
- [40] C. Haffner, W. Heni, Y. Fedoryshyn, J. Niegemann, A. Melikyan, D. L. Elder, B. Baeuerle, Y. Salamin, A. Josten, U. Koch, et al., *Nat. Photonics* **2015**, *9*, 1–5.
- [41] L. R. Dalton, P. A. Sullivan, D. H. Bale, *Chem. Rev.* **2010**, *110*, 25–55.
- [42] H. Xu, D. Yang, F. Liu, M. Fu, S. Bo, X. Liu, Y. Cao, *Phys. Chem. Chem. Phys.* **2015**, *17*, 29679–29688.
- [43] I. V. Kityk, R. I. Mervinskii, J. Kasperczyk, S. Jossi, *Mater. Lett.* **1996**, *27*, 233–237.
- [44] E. Gondek, J. Nizioł, A. Danel, M. Kucharek, J. Jędryka, P. Karasiński, N. Nosidlak, A. A. Fedorchuk, *Dyes Pigm.* **2019**, *162*, 741–745.
- [45] A. A. Fedorchuk, Y. I. Slyvka, E. A. Goresnik, I. V. Kityk, P. Czaja, M. G. Mys’kiv, *J. Mol. Struct.* **2018**, *1171*, 644–649.
- [46] Gaussian 16, Revision A.03, M. J. Frisch, G. W. Trucks, H. B. Schlegel, G. E. Scuseria, M. A. Robb, J. R. Cheeseman, G. Scalmani, V. Barone, G. A. Petersson, H. Nakatsuji, X. Li, M. Caricato, A. V. Marenich, J. Bloino, B. G. Janesko, R. Gomperts, B. Mennucci, H. P. Hratchian, J. V. Ortiz, A. F. Izmaylov, J. L. Sonnenberg, D. Williams-Young, F. Ding, F. Lipparini, F. Egidi, J. Goings, B. Peng, A. Petrone, T. Henderson, D. Ranasinghe, V. G. Zakrzewski, J. Gao, N. Rega, G. Zheng, W. Liang, M. Hada, M. Ehara, K. Toyota, R. Fukuda, J. Hasegawa, M. Ishida, T. Nakajima, Y. Honda, O. Kitao, H. Nakai, T. Vreven, K. Throssell, J. A. Montgomery, Jr., J. E. Peralta, F. Ogliaro, M. J. Bearpark, J. J. Heyd, E. N. Brothers, K. N. Kudin, V. N. Staroverov, T. A. Keith, R. Kobayashi, J. Normand, K. Raghavachari, A. P. Rendell, J. C. Burant, S. S. Iyengar, J. Tomasi, M. Cossi, J. M. Millam, M. Klene, C. Adamo, R. Cammi, J. W. Ochterski, R. L. Martin, K. Morokuma, O. Farkas, J. B. Foresman, and D. J. Fox, Gaussian, Inc., Wallingford CT, **2016**.
- [47] MOPAC2016, Version: 18.184W, James J. P. Stewart, Stewart Computational Chemistry, web: <http://OpenMOPAC.net>.
- [48] K. Aggarwal, J. M. Khurana, *Spectrochim. Acta, Part A* **2015**, *143*, 288–297.

## 6. List of Student's Published Works

- **Articles in impacted journals (associated with the dissertation)**

1. P. Solanke, S. Achelle, N. Cabon, O. Pytela, A. Barsella, B. Caro, F. Robin-le Guen, J. Podlesný, M. Klikar, F. Bureš, *Dyes Pigm.* **2016**, *134*, 129–138.
2. J. Podlesný, O. Pytela, M. Klikar, V. Jelínková, I. V. Kityk, K. Ozga, J. Jedryka, M. Rudysh, F. Bureš, *Org. Biomol. Chem.* **2019**, *17*, 3623–3634.

- **Articles in impacted journals (other)**

J. Podlesný, L. Dokládalová, O. Pytela, A. Urbanec, M. Klikar, N. Almonasy, T. Mikysek, J. Jedryka, I. V. Kityk, F. Bureš, *Beilstein J. Org. Chem.* **2017**, *13*, 2374 – 2384.

- **Presented lectures**

J. Podlesný, Y. Shirai; Design and synthesis of organic semiconductors based on thiophene derivatives as a hole transporting material for perovskite solar cells; National Institute of Materials Science – University of Pardubice Joint workshop; Tsukuba, Japan, 24. 3. 2016.

- **Presented posters**

1. J. Podlesný, F. Bureš, 2,5-Dihydropyrrolo[3,4-*c*]pyrrole-1,4-diones with peripheral substituents, 49<sup>th</sup> Advances in Organic, Bioorganic and Pharmaceutical chemistry, Lázně Bělohrad, 7. – 9. 11. 2014.
2. J. Podlesný, F. Bureš, 3,6-Disubstituované deriváty 2,5-dihydropyrrolo[3,4-*c*]pyrrol-1,4-dionu , 68. Sjezd Chemiků, Praha, 4. – 7. 9. 2016.
3. J. Podlesný, F. Bureš, Push-Pull chromofory s motivem thieno[3,2-*b*]thiofenu, 69. Zjazd chemikov, Vysoké Tatry – Horný Smokovec, Slovensko, 11. – 15. 9. 2017.
4. J. Podlesný, F. Bureš, Thieno[3,2-*b*]thiofen a thieno[2,3-*b*]thiofen jako elektron-donorní jednotky push-pull chromoforů, 70. Sjezd Chemiků, Zlín, 9. – 12. 9. 2018.